

Quantum Chemistry Study of the Interactions of Li⁺, Cl⁻, and I⁻ Ions with Model Ethers

Grant D. Smith*

Department of Chemical Engineering, University of Missouri—Columbia, Columbia, Missouri 65211

Richard L. Jaffe and Harry Partridge

NASA Ames Research Center, Moffett Field, California 94035

Received: May 16, 1996; In Final Form: October 1, 1996[⊗]

The geometries and energies of complexes of Li⁺, Cl⁻, and I⁻ with methane and model ether molecules have been studied using ab initio electronic structure calculations. For Li⁺, a [5s3p2d] basis set which accurately describes core electrons was derived. For Cl⁻, basis sets as large as [8s7p4d1f] were considered, while for I⁻ an 2sp1d ECP basis set augmented by a set of diffuse functions as large as [5sp4d1f] was employed. Calculations were performed at the SCF and MP2 levels of theory, and the effects of basis set superposition error on binding energies were considered. For the methane and ether molecules both D95** and cc-pVTZ basis sets with additional diffuse s and p functions were employed. The binding energies of Li⁺ to methane, dimethyl ether, and *ttt* 1,2-dimethoxyethane (DME) are found to be around 10, 40, and 40 kcal/mol, respectively. The binding energy of Li⁺ to *tgt* DME is approximately 60 kcal/mol due to the favorable interaction of Li⁺ with both DME oxygen atoms. The binding of Cl⁻ and I⁻ to dimethyl ether is much weaker, around 5–7 kcal/mol. A simple atomistic force field with two-body potential functions representing polarization effects is found to reproduce the ab initio complex energies quite well for the single ligand complexes. Polarization effects contribute significantly to the binding of Li⁺ to the neutral molecules, while the polarization effects in Cl⁻ and I⁻ complexes with dimethyl ether are relatively weak. The two-body force field accounts only partially for the decrease in binding per ligand in Li⁺–[O(CH₃)₂]_n complexes with the number of ligands as observed in the quantum chemistry calculations.

Introduction

The interactions of ions with neutral molecules are of great interest in a wide range of applications. For example, the characteristic manner in which ions are coordinated by ether molecules gives rise to the performance of crown ethers in separations and of poly(alkyl ethers) such as poly(oxyethylene) (POE) as polymer electrolytes. In these applications, it is widely believed that the ether or polyether interacts strongly with the cation, but only weakly with the anion. It is also believed that the ion–ether interactions control thermodynamic properties, such as solubility of the salt, and transport properties, such as the ion mobilities.

For the present study we have chosen LiCl and LiI as prototype lithium salts. We have used ab initio quantum chemistry calculations to determine the geometric preferences and energies for Li⁺–[O(CH₃)₂]_n, *n* = 1, 4, and Li⁺–(1,2-dimethoxyethane) (DME) complexes. Quantum chemistry results are compared with experimental data where the latter are available. Additionally, we have employed quantum chemistry in the study of Li⁺–Li⁺, Li⁺–Cl⁻, Li⁺–I⁻, Cl⁻–Cl⁻, and I⁻–I⁻ as well as complexes between Cl⁻ and I⁻ and dimethyl ether.

One goal for the present study is to obtain an atomistic force field that can be used to describe the intramolecular and intermolecular interactions in lithium salt–POE solutions for use in molecular dynamics simulations of polymer electrolytes. Based upon the quantum chemistry calculations, we have parametrized potential energy functions describing the molecule–molecule, ion–molecule, and ion–ion interactions in LiCl/ether and LiI/ether systems. Our intention is to combine these potential energy functions with our previously determined force

field for POE¹ for use in modeling polymer electrolytes. This force field for POE is based upon quantum chemistry calculations of the conformational energies and geometries of diethyl ether and DME^{1,2} and molecular mechanics calculations on polyethers.³ The POE force field has subsequently been used successfully in molecular dynamics simulations of gas- and liquid-phase DME⁴ and POE melts.^{5,6}

Polarization Effects

Of particular interest to us are the importance of polarization effects in the interactions of ions with the model ethers and the ability of simple pairwise additive potential energy functions to reproduce the energies of these complexes. It has been long recognized that polarization or induction effects are important in the interactions between ions and between ions and neutral molecules. In an ion pair, each ion will polarize, i.e., induce dipole and higher order moments in, the other ion. Considering only dipole polarization, the polarization energy (in kcal/mol) for a monovalent ion pair is given by⁷

$$E_{jk}^{\text{pol}} = -332.07[\alpha_j + \alpha_k]/2r_{jk}^4 + O(r_{jk}^{-7}) + \dots \quad (1)$$

where the ion dipole polarizabilities (in Å³) are α_j and α_k and r_{ij} is the interionic separation (in Å). The factor of 2 in the denominator of the first term accounts for the work of polarization. The induced dipole moment in ion *j* also interacts with the induced dipole moment in ion *i*, and the induced dipoles themselves are a function of the induced dipole moment in the other ion. These effects lead to the higher order terms in inverse *r*. This form of E_{jk}^{pol} , when combined with the r^{-1} Coulomb term and a steric repulsion term, has been found to describe the ionic bond energy of alkali halide molecules quite well.⁷

[⊗] Abstract published in *Advance ACS Abstracts*, December 1, 1996.

Equation 1 can be modified to consider the interaction of a pair of atoms j and k with partial atomic charges q_j and q_k and atomic polarizabilities α_j and α_k , respectively. Considering only the lowest order term, the polarization energy is

$$E_{jk}^{\text{pol}} = -332.07[q_k^2\alpha_j + q_j^2\alpha_k]/2r_{jk}^4 = -D_{jk}/r_{ij}^4 \quad (2)$$

The strength of the interaction is linearly dependent on the atomic polarizabilities and quadratically dependent upon the atomic charges. Therefore, when an ion interacts with a neutral atom or an atom with a small partial charge, the polarization energy can still be quite large, depending upon the separation distance and the polarizability of the neutral or partially charged atom.

Equation 2 is a two-body expression for the polarization energy. Two-body potential functions for nonbonded interactions are commonly used in representations of the potential energy of many atom systems, primarily for reasons of computational expediency. In such a force field, the nonbonded energy (in kcal/mol) due to interactions between atoms i and j is often considered to be the pairwise sum of repulsion, dispersion, and electrostatic interactions of the form

$$E_{ij}(r_{ij}) = A_{ij} \exp(-B_{ij}r_{ij}) - \frac{C_{ij}}{r_{ij}^6} + \frac{332.07q_iq_j}{r_{ij}} \quad (3)$$

where A_{ij} , B_{ij} , and C_{ij} are repulsion/dispersion parameters, q_i and q_j are the atomic charges, and r_{ij} is the atomic separation in angstroms. In the spirit of the simple two-body force field representation, the polarization interaction of an ion j with a polyatomic molecule can be considered to be given by

$$E_j^{\text{pol}} = -\sum_k D_{jk}/r_{jk}^4 \quad (4)$$

where the sum is over the atoms comprising the polyatomic molecule.

Equation 4 accounts approximately for two-body polarization effects between the ion and the molecule but neglects the interactions between induced dipoles within the molecule and the influence of these mutual induction effects on the interaction between the molecule and the ion. These are many body-effects; i.e., the interactions of the ion with any atom of the molecule are influenced by its interaction with the other atoms. Polarizable models which attempt to account for these many-body polarization effects are available and have been applied in simulations involving the interaction of ions with simple molecules, including $\text{Li}^+-\text{H}_2\text{O}$.⁸ Unfortunately, these approaches take 2–4 times as much computational effort as nonpolarizable models.⁹ This is a serious limitation, particularly when applied to polymer systems where simulations usually contain several to 100 times as many atoms as those of simple molecular systems. Many thousands or tens of thousands of atoms need to be considered in simulations of polymer electrolytes. Because of the expense involved with polarizable models, we desired to determine the magnitude of polarization effects in the interaction of Li^+ with halide ions and in the interactions of these ions with model ethers. In addition, we have investigated the suitability of the simple two-body potential of the form given by eq 4 to represent the polarization effects between the ions and the model molecules.

Quantum Chemistry Calculations

All quantum chemistry calculations in this study were performed using the quantum chemistry codes Gaussian92¹⁰ and Mulliken¹¹ at the NASA Ames Research Center and Mulliken at the University of Missouri—Columbia. Calculations were performed on a Cray C-90 and on IBM RS6000 workstations.

TABLE 1: [8s5p3d/5s4p2d] Basis Set for Li

exponent	coefficients				
	Shell s				
1360.306	0.000844	0.0	0.0	0.0	0.0
204.1193	0.006491	0.0	0.0	0.0	0.0
46.45243	0.032691	0.0	0.0	0.0	0.0
13.10943	0.119676	0.0	0.0	0.0	0.0
4.189925	0.0	1.0	0.0	0.0	0.0
1.434060	0.0	0.0	1.0	0.0	0.0
0.509171	0.0	0.0	0.0	1.0	0.0
0.203668	0.0	0.0	0.0	0.0	1.0
Shell p					
10.0	0.150873	0.0	0.0		
4.0	0.372952	0.0	0.0		
1.6	0.0	1.0	0.0		
0.3079	0.0	0.0	1.0		
Shell d					
8.53815	0.277606	0.0			
3.41526	0.785589	0.0			
0.6573	0.0	1.0			

TABLE 2: Diffuse Functions Added to the cc-pVTZ Basis Sets for Cl and Ar and the ECP 2sp1d Basis Set for I and Xe

shell	exponent			
	Cl	Ar	I	Xe
s	0.05417	0.06513		
s	0.01806	0.02171		
p	0.04337	0.0515		
p	0.01446	0.0172		
d	0.11467			
sp			0.026	0.0282
sp			0.009	0.0094
sp			0.003	
d			0.089	0.092
d			0.030	0.031
d			0.010	
f			0.319	0.356

Lithium Basis Set. Earlier work on alkali chlorides has demonstrated that quantum chemistry calculations can accurately reproduce experimental values for the dissociation energy and ground state separation and vibrational frequency for LiCl .¹² This study utilized an extended Slater basis set of the form $\text{Li}[6s8p6d2f]$ and $\text{Cl}[7s6p3d2f]$. We find that standard double-zeta D95¹³ and triple-zeta 6-311G¹⁴ basis sets give poor descriptions of Li^+ due to their poor descriptions of the Li core electrons, leading to very large basis set superposition errors (>3 kcal/mol) in complexes involving Li^+ and poor representation of the binding energies and equilibrium geometries in these complexes. Therefore, we have derived a new Li basis set of the form [8s4p3d/5s3p2d] which has a much improved description of the Li core electrons. The exponents and contraction coefficients for this basis set are given in Table 1.

Anion and Ligand Basis Sets. We found that accurate representation of the experimental bond energy and ground state bond length in LiCl resulted when a triple-zeta polarized basis set for Cl with additional s, p, and d diffuse functions was utilized. The basis set was derived by adding two sets of diffuse s and p and a single set of diffuse d functions to the correlation consistent TZP (cc-pVTZ) basis set for Cl.¹⁵ The contraction coefficients and exponents for the additional diffuse functions for the resulting [17s113d1f/7s6p3d1f] Cl basis set, labeled cc-pVTZ+2s2pd, are shown in Table 2. For LiI , we found accurate representation of the experimental bond energy and ground state bond length using an augmented version of the effective core potential (ECP) of Stevens et al.¹⁶ The [5sp1d/2sp1d] valence orbital description for this basis set was augmented by three sets of diffuse sp, three sets of diffuse d, and a set of f functions.

TABLE 3: LiCl and LiI Dissociation Energies as a Function of Basis Set

basis set			energy ^a		BSSE	
Li ⁺	Cl ⁻ /I ⁻	geometry, Å	SCF	MP2	SCF	MP2
LiCl						
[5s2p1d] ^b	D95+*	2.098 (SCF)	140.7			
[5s2p1d]	D95+*	2.101 (SCF)	140.7	140.0	0.025	0.653
[5s2p1d]	[6s5p3d1f] ^c	2.101 (SCF)	144.6	144.1		
[5s2p1d]	[7s6p3d1f] ^d	2.101 (SCF)	147.5	146.7		
[5s2p1d]	[8s7p4d1f] ^e	2.101 (SCF)	147.5	146.7		
[5s3p1d] ^f	[7s6p3d1f]	2.038 (MP2)	151.2	151.4		
[5s3p2d] ^g	[7s6p3d1f]	2.035 (MP2)	151.7	152.6	0.011	0.723
exp		2.02		153.2		
LiI						
[5s3p1d]	[4sp3d] ^h	2.402 (MP2)	133.1	133.0	0.088	0.927
[5s3p1d]	[5sp4d1f] ⁱ	2.398 (MP2)	133.7	134.2	0.090	0.741
exp		2.392		135.2		

^a Dissociation energy D_e , measured with respect to the ionic species Li⁺ and Cl⁻ or I⁻ at infinite separation, in kcal/mol, without BSSE correction. ^b Basis set given in Table 1 minus the most diffuse set of p and d functions. ^c cc-pVTZ basis set plus diffuse functions given in Table 2 minus the most diffuse set of s and p functions. ^d cc-pVTZ basis set plus diffuse functions given in Table 2. ^e Basis set given in Table 2 plus a set of diffuse s, p, and d functions. Exponents are one-third of the value of the most diffuse exponents given in the table. ^f Basis set given in Table 1 minus the most diffuse set of d functions. ^g Basis set given in Table 1. ^h Basis set given in Table 2 minus the most diffuse set of sp, d, and f functions. ⁱ Basis set given in Table 2.

The exponents for the diffuse functions for the resulting [8sp4d1f/5sp4d1f] valence basis set are given in Table 2. For the ligand basis sets, the D95 set augmented by diffuse and polarization functions (denoted D95+**) and the cc-pVTZ set were used. These basis sets are discussed in greater detail below.

Lithium Chloride and Lithium Iodide

Quantum Chemistry. The dissociation or binding energy D_e of LiCl and LiI, relative to the infinitely separated ions, is given, as a function of basis set, in Table 3. Experimental data are also given in the table, as obtained from the relationship¹²

$$D_e = D_e(\text{neutral}) + \text{IP}(\text{Li}) - \text{EA}(\text{Cl or I}) \quad (5)$$

where $D_e(\text{neutral})$ is the dissociation energy of LiCl or LiI to neutral atoms,¹⁷ IP(Li) is the ionization potential for Li,¹⁸ and EA(Cl or I) is the electron affinity of chlorine or iodine.¹⁹ Calculations for LiCl and LiI were performed at the SCF level and at the MP2 level of electron correlation treatment. Little difference was found between SCF and MP2 binding energies for all basis sets investigated, indicating that dispersion effects are not important in the binding of LiCl. For selected cases, the BSSE corrections, which were small for LiCl and LiI when adequate basis sets are used, are given in Table 3.

With the best basis sets investigated, the calculated LiCl binding energy is in quite good agreement with experiment, as shown in of Table 3. By comparing the computed binding energy for systematic changes in the Li and Cl basis sets, we can identify those basis functions making significant contributions to the binding. Table 3 shows that a considerable increase in the LiCl binding energies results from improving the representation of Cl to TZP with a set of diffuse s and p functions from DZP with a set of diffuse s and p functions. Further increases in the binding energy result when an additional set of diffuse s and p functions is included for Cl. Further improvements of the Cl basis set beyond that given in Table 2, however, had no significant effect on the LiCl binding energy. It is clear that the most diffuse p and d functions are important in the representation of Li. Further improvement of the Li basis

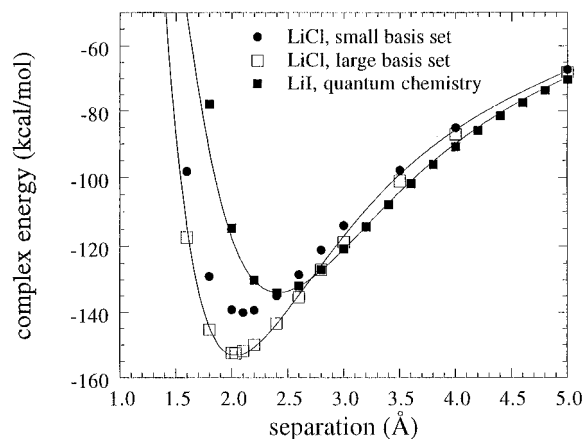


Figure 1. Complex energies of LiCl and LiI as a function of separation, relative to the ions at infinite separation. Quantum chemistry energies are MP2 values using a (large) [5s3p2d]/[7s6p3d1f] [Li/Cl] basis set, a (small) [5s2p1d]/[D95+*] [Li/Cl] basis set, and a [5s3p2d]/[4sp3d]-ECP [Li/I] basis set. Also shown are energies from the force field potential functions. Solid lines are cubic spline interpolations.

set did not significantly change the LiCl binding energy. For LiI, the final set of diffuse d functions and the set of f functions for I made only a small contribution to the binding.

Employing the Li[5s3p2d], the Cl[7s6p3d1f], and the I[4sp3d]-ECP basis sets, the energy of LiCl and LiI were determined as a function of interatomic separation. The MP2 complex energies (which differ little from the SCF energies), relative to the ions at infinite separation, are shown in Figure 1. For comparison, energies obtained using the smaller Li[5s2p2d] and Cl[D95+*] basis sets, referred to as the small basis set energies, are also shown in Figure 1.

Potential Energy Functions. In determining the parameters for the two-body potential functions for LiCl and LiI (eqs 2 and 3), the dispersion parameters C_{LiCl} and C_{LiI} were set to zero since dispersion effects are small due to the low polarizability of Li⁺. The polarizability of Li⁺ is negligible compared to that of Cl⁻ or I⁻ and was assigned a value of zero for the purpose of fitting the LiCl and LiI potentials. Hence, D_{LiCl} and D_{LiI} (eq 2) depend only on the polarizabilities of the anions. The parameters A_{LiCl} , B_{LiCl} , and D_{LiCl} and A_{LiI} , B_{LiI} , and D_{LiI} which yielded the best agreement between the calculated potentials and the quantum chemistry energies as determined by standard nonlinear least-squares fitting methods are given in Table 4. The resulting potentials are shown in Figure 1. Agreement with quantum chemistry energies is good, particularly near the equilibrium separations. Subtracting the Coulomb energy, given by

$$E_{\text{coulomb}} (\text{kcal/mol}) = \frac{332.07q_iq_j}{r_{ij}} = \frac{-332.07}{r_{ij}} \quad (6)$$

from the quantum chemistry and force field energies yields the net repulsion plus dispersion plus polarization contribution to the complex energies, as shown in Figure 2. Agreement between the force field and quantum chemistry energies for this quantity is reasonable, indicating that the simple representation of repulsion and polarization terms given in eqs 3 and 4 is adequate. The difference between the force field and quantum chemistry energies is on the order of the uncertainties (due to finite basis set, electron correlation, and BSSE effects) in the quantum chemistry energies. Inclusion of higher order polarization terms did not improve agreement with the quantum chemistry energies.

Coulombic and steric repulsion effects are not expected to differ significantly between the small and large basis sets used in our calculations for LiCl. Therefore, differences in the complex energies between the small and large basis set

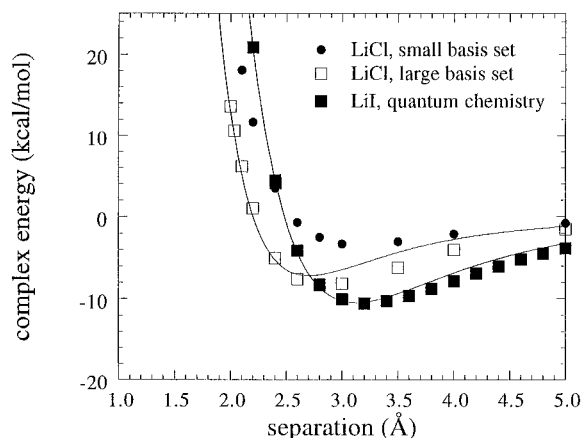


Figure 2. Same as Figure 1 after subtraction of the Coulomb interaction energy.

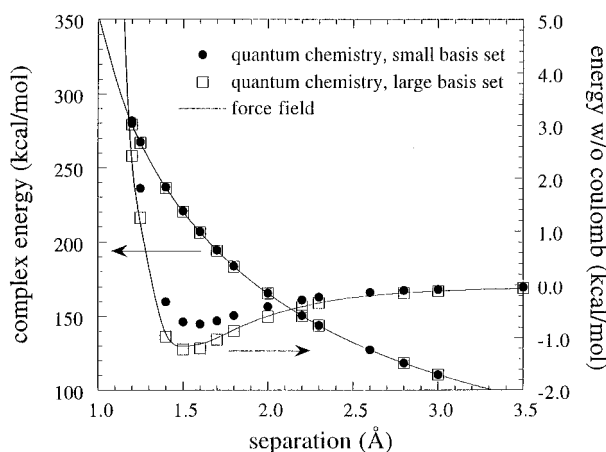


Figure 3. Complex energy of $\text{Li}^+ - \text{Li}^+$ as a function of separation, relative to the ions at infinite separation. Quantum chemistry energies are MP2 values using a $\text{Li}[5s3p2d]$ (large) basis set and a $\text{Li}[5s2p1d]$ (small) basis set. Energies after subtraction of the Coulomb interaction are also shown. Also shown are energies from the force field potential function.

calculations can be attributed mainly to differences in polarization effects and indicate the importance of these contributions. For the small Cl basis set, the atomic polarizability (SCF) for Cl^- is 2.36 \AA^3 , while for the large basis set it is 4.14 \AA^3 at the SCF level and 4.64 \AA^3 at the MP2 level. From D_{LiCl} we obtain a dipole polarizability of 4.39 \AA^3 for Cl^- , in good agreement with the large basis set quantum chemistry prediction. This value is also in good agreement with the values obtained from a number of theoretical studies of Cl^- .²⁰ For I^- , our potential energy function yields a dipole polarizability of 12.7 \AA^3 , in reasonable agreement with the MP2 value for I^- of 10.4 \AA^3 obtained using the $\text{I}[4sp3d]$ ECP basis set.

$\text{Li}^+ - \text{Li}^+$

Using the larger $\text{Li}[5s3p2d]$ and the smaller $\text{Li}[5s2p1d]$ basis sets, the energy for a $\text{Li}^+ - \text{Li}^+$ complex was determined as a function of separation. The MP2 energies, relative to ions at infinite separation, are shown in Figure 3. For all separations greater than 1.5 \AA , the difference between the SCF and MP2 binding energies is less than 0.05 kcal/mol . BSSE error at both the SCF and MP2 level is negligible. As with LiCl and LiI , we conclude that dispersion interactions are not important in the $\text{Li}^+ - \text{Li}^+$ complex. Unlike LiCl , where significant differences in binding energy were seen between calculations using the small and large basis sets, little difference is seen in $\text{Li}^+ - \text{Li}^+$ complex between the two basis sets. This is consistent with the low polarizability of Li^+ . This can be seen in Figure 3,

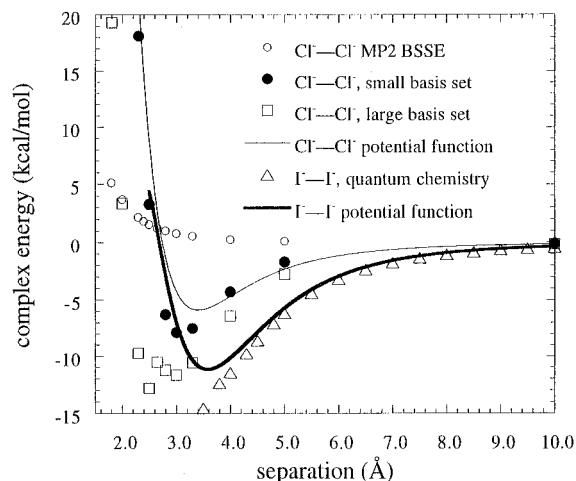


Figure 4. Complex energy of $\text{Cl}^- - \text{Cl}^-$ and $\text{I}^- - \text{I}^-$ as a function of separation, relative to the ions at infinite separation. Quantum chemistry energies are MP2 values using a $\text{Cl}[7s6p3d1f]$ (large), $\text{Cl}[D95+*]$ (small), and an $\text{I}[5sp4d1f]$ ECP basis set. Also shown are the BSSE energies for $\text{Cl}^- - \text{Cl}^-$ at the MP2 level using the large basis set. The force field potential function energies are also shown as solid lines.

TABLE 4: Force Field Parameters for Ion/Ion Interactions

pair	A, kcal/mol	B, \AA^{-1}	C, (kcal/mol) \AA^6	D, (kcal/mol) \AA^4
Alkali Halides				
$\text{Li}^+ - \text{Cl}^-$	30 868	3.134	0	729.4
$\text{Li}^+ - \text{I}^-$	23 625	2.437	0	2108.7
Other Interactions				
$\text{Li}^+ - \text{Li}^+$	44 195	7.277	0	9.30
$\text{Ar} - \text{Ar}$	160 677	3.5144	1329	0.0
$\text{Cl}^- - \text{Ar}$	58 734	2.945	1834	232.4
$\text{Cl}^- - \text{Cl}^-$	21 470	2.376	2530	1458.8
$\text{Xe} - \text{Xe}$	298 590	3.0056	6134	0
$\text{I}^- - \text{Xe}$	92 863	2.5218	11228	596.1
$\text{I}^- - \text{I}^-$	28 881	2.0380	205551	3453.6

where binding in the complex after subtraction of the Coulomb interaction, due to polarization interactions, is less than 1 kcal/mol . Using the large basis set MP2 value of 0.03 \AA^3 for the polarizability of Li^+ , to obtain D_{LiLi} the A_{LiLi} and B_{LiLi} parameters which give the best fit to the quantum chemistry are listed in Table 4. The resulting potential is shown in Figure 3. The potential is in excellent agreement with the quantum chemistry data.

$\text{Cl}^- - \text{Cl}^-$ and $\text{I}^- - \text{I}^-$

Quantum Chemistry for $\text{Cl}^- - \text{Cl}^-$ and $\text{I}^- - \text{I}^-$. The complex energies and BSSE for $\text{Cl}^- - \text{Cl}^-$ at the SCF and MP2 levels were calculated using the large $\text{Cl}[7s6p3d1f]$ and the small $\text{Cl}[D95+*]$ basis sets. Calculations were performed for $\text{I}^- - \text{I}^-$ using the $\text{I}[5sp4d1f]$ ECP basis set. The BSSE corrected MP2 complex energies, after subtracting Coulomb interactions (eq 5), are shown in Figure 4. The BSSE corrections for $\text{Cl}^- - \text{Cl}^-$ at the MP2 level (large basis set) are also shown. A much larger difference between the SCF and MP2 complex energies is seen in $\text{Cl}^- - \text{Cl}^-$ and $\text{I}^- - \text{I}^-$ than was found for LiCl , LiI , or $\text{Li}^+ - \text{Li}^+$. This, and the fact that the BSSE is much larger for the anion pairs than in the alkali halides or $\text{Li}^+ - \text{Li}^+$, indicates that dispersion effects are relatively large for the anion–anion interactions.

Ar and Xe Complexes. The binding in $\text{Cl}^- - \text{Cl}^-$ yielded by the large basis set calculations is much stronger than was found using the small basis set, as shown in Figure 4. At separations of less than about 3.5 \AA , a crossing from a $\text{Cl}^- - \text{Cl}^-$ path to a $[\text{Cl} - \text{Cl}]^- + e^-$ path occurs, accounting for the behavior of the MP2 interaction energy at small separations.

Similar effects are indicated by the increasingly large binding energies for I⁻-I⁻ with decreasing separation. Because of this behavior at short separations, force field parameters for Cl⁻ and I⁻ cannot be obtained directly from the anion complex energies. Therefore, we have examined Ar-Ar and Ar-Cl⁻ complexes using an cc-pVTZ+2s2pd basis set for Ar and Xe-Xe and Xe-I⁻ complexes using an [4sp3d]ECP basis set for Xe. The diffuse exponents for Ar and Xe are given in Table 2. The uncorrected and BSSE corrected MP2 complex energies for the Ar complexes and the BSSE corrected MP2 energies for the Xe complexes are shown in Figure 5. From a cubic spline interpolation, the BSSE corrected Ar-Ar complex energy has a minimum of -0.20 kcal/mol at a separation of 3.93 Å, while that for the Xe-Xe complex is -0.35 kcal/mol at 4.64 Å. The BSSE corrected Cl⁻-Ar complex has a minimum of -1.14 kcal/mol at 3.79 Å, while the minimum for the I⁻-Xe complex is -1.73 kcal/mol at 4.40 Å. The Cl⁻-Ar complex geometry is in good agreement with the value of 3.75 Å obtained by Ahlrichs et al.²⁰ using an ab initio based potential function. Our binding energy is somewhat less than the 1.48 kcal/mol obtained in that study.

The repulsion parameters *A* and *B*, the dispersion parameters *C*, and the polarization parameters *D* were treated as adjustable for the Ar-Ar, Ar-Cl⁻, Xe-Xe, and Xe-I⁻ complexes. The best representations of the quantum chemistry data by the potential functions are shown in Figure 5. The resulting parameters are given in Table 4. The repulsion parameters *A*_{ArCl⁻} and *B*_{ArCl⁻} are in good agreement with values of 56 588 kcal/mol and 2.986 Å⁻¹ obtained by Ahlrichs et al.²⁰ based upon an SCF level study of Ar-Cl⁻ complexes. From the parameters *D*_{ArCl⁻} and *D*_{XeI⁻}, dipole polarizabilities of 1.68 and 3.59 Å³ are obtained for Ar and Xe, respectively, in excellent agreement with experimental values²¹ 1.64 and 4.01 Å³.

Potential Functions for Cl⁻-Cl⁻ and I⁻-I⁻. Using standard arithmetic mean (*B*) and geometric mean (*A*, *C*) combining rules for the potential parameters, values of *A*, *B*, and *C* were determined for Cl⁻-Cl⁻ and I⁻-I⁻ from values for the Ar and Xe complexes, respectively. Values of *D*_{Cl⁻-Cl⁻} and *D*_{I⁻-I⁻} were obtained using Cl⁻ and I⁻ dipole polarizabilities of 4.39 and 10.4 Å³, respectively (see above). The potential parameters are given in Table 4. The resulting Cl⁻-Cl⁻ and I⁻-I⁻ potentials (without Coulomb contribution) are shown in Figure 4. The calculated potentials agree well with the respective anion pair quantum chemistry complex energies at larger separations, where the path crossing effects are unimportant.

Li⁺-Complexes with Methane and Model Ethers

The first step in our study of the complexes of Li⁺ with model ethers was to investigate the influence of the Li and ether basis set on the energy of a Li⁺/dimethyl ether complex with C_{2v} symmetry, as illustrated in Figure 6 (Li⁺-dimethyl ether structure I). These results are shown in Table 5. The experimental complex energy from ion cyclotron resonance spectroscopy (ICR)²² is also given in the table. The complex energy is more strongly dependent upon the Li basis set than the ether basis set for reasons that are unclear. Differences between SCF (not shown) and MP2 energies are small, indicating dispersion interactions are not important in the Li⁺-ether interaction. The BSSE correction is somewhat larger than in LiCl, indicative of some remaining deficiencies in the basis set, but it is small compared to the total binding energy and, more importantly, the computed and experimental binding energies (see below) are in excellent agreement. The Li[5s3p2d] basis set with the D95+** ether basis set results in a satisfactory description of the Li⁺-dimethyl ether complex energy, i.e., in good agreement with experiment and with calculations using

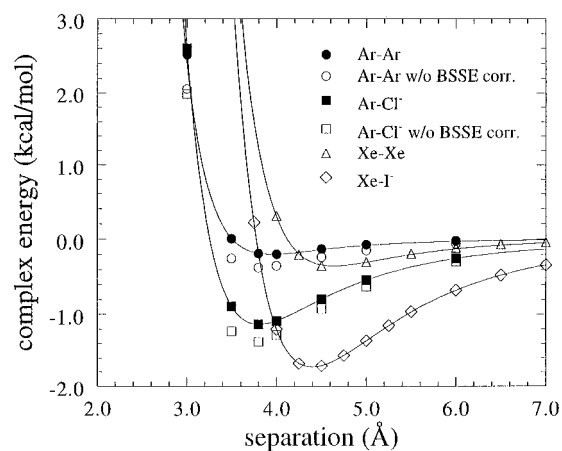


Figure 5. Complex energy of Ar-Ar, Ar-Cl⁻, Xe-Xe, and Xe-I⁻ as a function of separation, relative to the ions at infinite separation. Quantum chemistry energies are MP2 values using Cl[7s6p3d1f], Ar[6s5p2d1f], I[5sp4d1f ECP], and Xe[4sp3d ECP] basis sets. Energies with and without BSSE correction are shown for the Ar complexes. Solid lines are energies from the force field potential.

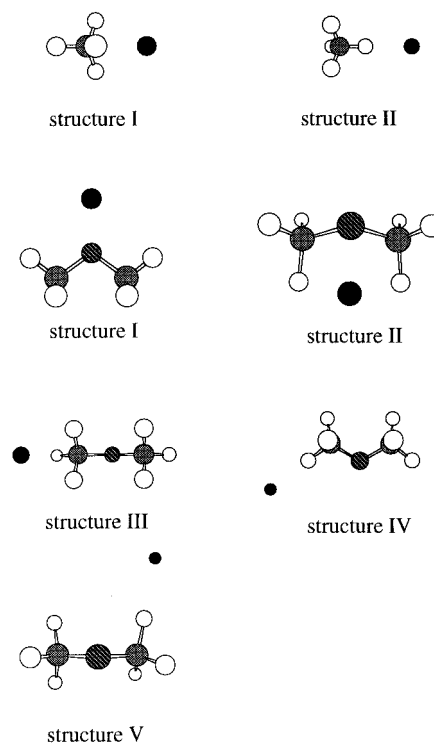


Figure 6. Geometries of the Li⁺-methane and Li⁺-dimethyl ether complexes investigated.

larger basis sets. Therefore, these basis sets were used in the studies of Li⁺ with model ethers and methane described below. The smaller Li[5s2p1d] basis set was used in geometry optimizations (except for Li⁺-methane), as it was found that the additional d functions in the Li[5s3p2d] basis set made very little difference in the optimized geometries.

The computed dissociation energy (*D*_e) of the Li⁺-dimethyl ether complex, as given in Table 5, is 38.4 kcal/mol (39.8 kcal/mol if the smaller basis set is used). In this complex, the Li⁺-O separation is 1.835 Å, the ether C-O bond length is 1.453 Å, and the C-O-C bond angle is 110.6°, as compared to the respective values 1.418 Å and 110.9° in the isolated ether. These distortions in the ether geometry result in a 1.4 kcal/mol increase in the ether energy. From MP2 Mulliken population analysis, we also find the oxygen partial charge changes from -0.22 to -0.58, and the carbon partial charge changes from -0.27 to -0.16 upon complex formation.

TABLE 5: Ion–Molecule Complex Energies as a Function of Basis Set

distance, Å	geometry [Li ⁺ or Cl ⁻ /ligand]	energy, kcal/mol			
		[Li ⁺ or Cl ⁻ /ligand]	MP2	BSSE	corr
Dimethyl Ether (Li ⁺ -O) Structure I					
1.835	[5s2p1d/D95+**] MP2	[5s2p1d/D95+**]	-37.32		
1.835	[5s2p1d/D95+**] MP2	[5s3p2d/D95+**]	-40.74	1.02	-39.72
1.835	[5s2p1d/D95+**] MP2	[5s3p2d/cc-pVTZ+sp] ^a	-39.32	0.91	-38.41
exp					-40.6 ^b
Methane (Li ⁺ -C) Structure I					
2.10	[5s3p2d/D95+**] MP2	[5s3p2d/D95+**]	-10.96	0.30	-10.66
Methane (Li ⁺ -C) Structure II					
2.99	[5s3p2d/D95+**] MP2	[5s3p2d/D95+**]	-4.54	0.16	-4.38
1,2-Dimethoxyethane <i>tgt</i> (Li ⁺ -O)					
1.870	[5s3p2d/D95+**] MP2	[5s3p2d/D95+**]	-66.23	2.83	-63.40
1.870	[5s3p2d/D95+**] MP2	[5s3p2d/cc-pVTZ+sp]	-60.36	0.79	(-61.21) ^c
exp					-59.56
					(-57.37) ^c
exp					-57.6 ± 4.4 ^d
1,2-Dimethoxyethane <i>ttt</i> (Li ⁺ -O)					
1.837	[5s2p1d/D95+**] MP2	[5s3p2d/D95+**]	-41.36	1.60	-39.76
Dimethyl Ether (Cl ⁻ -O)					
4.30 ^e	[D95+*/D95+**] MP2	[cc-pVTZ+2s2p1d ^a /D95+**]	-7.34	0.68	-6.66
4.30	[D95+*/D95+**] MP2	[cc-pVTZ+3s3p2d ^a /D95+**]	-7.56	0.88	-6.68
4.30	[D95+*/D95+**] MP2	[cc-pVTZ+3s3p2d ^a /cc-pVTZ+sp] ^a	-8.01	1.21	-6.90

^a Diffuse exponents are determined by successively taking the exponent for the most diffuse function and dividing by 3. ^b Extracted from experimental ΔG_{298} (ref 22) using thermodynamic parameters for the present work. ^c ΔH°_0 determined using thermodynamic parameters from the present work. ^d ΔH°_0 from the experiments of ref 24. ^e Minimum from MP2 optimized geometry. After BSSE correction, the minimum is closer to 4.55 Å and about 0.2 kcal/mol deeper.

In order to compare the calculated D_e with the measured ΔG°_{298} ²² for the Li⁺-dimethyl ether complex, we computed the harmonic normal mode vibration frequencies for dimethyl ether and its complex with Li⁺. These frequencies were determined at the MP2 level using the D95+** ether and [5s2p1d] Li⁺ basis sets and scaled by 0.94 to adjust for the effect of anharmonicity. The vibrational zero point energy correction is 1.46 kcal/mol, which yields a value of 36.9 kcal/mol for D_0 . The biggest differences between this work and that of ref 22 are the frequencies of the three Li⁺-ether complex vibrations. We obtain values of 515, 134, and 128 cm⁻¹, while Woodin and Beauchamp²² used 554, 450, and 390 cm⁻¹, the values computed for the Li⁺-H₂O complex.²³ The translational, vibrational, and rotational contributions to ΔH°_{298} and ΔS° were calculated according to standard formulas. The thermal vibrational energy is 1.02 kcal/mol, making $\Delta H^{\circ}_{298} = -35.9$ kcal/mol. Based on the quantum chemistry data, the vibrational and rotational contributions to the entropy are 6.71 and 1.83 cal/(mol deg), respectively (Woodin and Beauchamp²² report 2.34 and 1.78). As a result, our best value for the free energy for the complex formation, ΔG°_{298} , is -29.1 kcal/mol compared to the value -31.3 obtained by the ICR experiment.²² Conversely, if one starts with the experimental free energy and uses our data for the thermodynamic analysis, the limiting value of D_e is -40.6 kcal/mol and ΔH°_{298} is -38.1 kcal/mol.

Li⁺-Methane

Quantum Chemistry. In order to better understand the importance of the Li⁺-O interaction in Li⁺-ether complexes, and to independently determine Li⁺-H parameters for the force field, we examined Li⁺-methane complexes of the two C_{3v} structures shown in Figure 6. The equilibrium complex energies, relative to the infinitely separated relaxed species, are given in Table 5. The intermolecular nonbonded energy as a function of the C-Li⁺ separation along the symmetry axis for the two structures is shown in Figure 7. The Li⁺-methane energies were not corrected for BSSE because of the small size of this correction. For each fixed C-Li⁺ separation, the methane geometry was allowed to “distort” so as to minimize

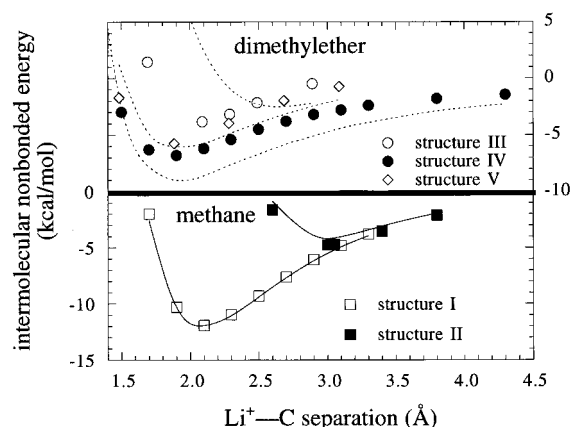


Figure 7. Intermolecular nonbonded energy for the Li⁺-methane and Li⁺-dimethyl ether complexes using Li[5s3p2d] and D95+** ligand basis sets. Lines for the methane (solid) and dimethyl ether (dashed) energies are values from the force field potential.

the complex energy. The energies in Figure 7 are relative to the *distorted* methane geometries and ion at infinite separation and hence represent the intermolecular nonbonded interactions between methane and Li⁺ for the various geometries. The intermolecular nonbonded energy will be greater than the complex energy, which is measured relative to the relaxed geometry of the isolated methane molecule, by the “distortion energy” of the methane. The distortion energy is given by the energy of the isolated methane in the distorted geometry relative to that in the relaxed geometry. The distortion energy is greater for the sterically strained configurations corresponding to shorter ion-molecule separations and ranges from a few tenths of a kcal/mol to about 2 kcal/mol for the complexes.

Potential Energy Functions. Due to mutual induction effects, the intermolecular nonbonded energies shown in Figure 7 also include interactions between induced dipole moments within the methane molecule. In the two-body description of the potential function given by eqs 2-4, this energy must be accounted for through *ij* terms involving the ion (*i*) and the

TABLE 6: Force Field Parameters^a for Interactions of Li⁺, Cl⁻, and I⁻ with Neutral Molecules

pair	A, kcal/mol	B, Å ⁻¹	C, (kcal/mol) Å ⁶	D, (kcal/mol) Å ⁴
Methane				
Li ⁺ -H	13 139	4.376	0	94.1 (0.567) ^b
Li ⁺ -C	14 192	3.879	0	0.0 (0.000)
Ethers				
Li ⁺ -H	13 139	4.376	0	77.4 (0.466)
Li ⁺ -C	8 140	2.632	0	473.2 (2.850)
Li ⁺ -O	191 106	5.711	0	76.9 (0.463)
Cl ⁻ -C	17 926	2.733	1273.3	67.2 (0.361)
Cl ⁻ -O	40 353	3.220	1005	536.3 (2.492)
Cl ⁻ -H	7 543	3.058	263	0.0 (0.000)
I ⁻ -C	23 213	2.462	3301	77.7 (0.361)
I ⁻ -O	52 238	2.949	2604	712.4 (2.492)
I ⁻ -H	9 764	2.787	682.5	0.0 (0.000)
C-C ^c	14 976	3.090	640.8	0
C-O ^c	33 702	3.577	505.6	0
C-H ^c	4 320	3.415	138.2	0
O-O ^c	75 845	4.063	398.9	0
O-H ^c	14 176	3.902	104.5	0
H-H ^c	2 650	3.74	27.4	0

^a Parameters to be used in evaluating eqs 2 and 3. ^b Numbers in parentheses are effective atomic polarizabilities for the H, C, or O atom. ^c Parameters from ref 1, to be used for intermolecular ether-ether interactions.

atoms comprising the methane (*j*); hence, for our purpose the mutual induction effects contribute to the effective intermolecular potential. In fitting the Li⁺-methane potential A_{HLi} , B_{HLi} , A_{CLi} , B_{CLi} , α_{H} , and α_{C} were treated as adjustable parameters. The "effective" atomic polarizabilities α_{H} , and α_{C} , used in determining D_{HLi} and D_{CLi} , are not atomic polarizabilities in the sense of those determined for the diatomic complexes above. Rather, these are values which allow the best represent of the Li⁺-methane polarization effects in the context of the force field given by eqs 2-4. The dispersion parameters C_{ij} and the polarizability of Li⁺ were set to zero. Partial atomic charges from quantum chemistry electrostatic potential calculations of $q_{\text{H}} = 0.09$ kcal/mol and $q_{\text{C}} = -0.36$ kcal/mol were used for methane. Figure 7 shows the resulting intermolecular nonbonded potential from the force field for Li⁺-methane. The representation of the quantum chemistry complex energies by the force field is quite good. The resulting force field parameters are given in Table 6. For the lowest energy configuration (structure I with a Li⁺-separation of 2.1 Å), the contributions of the dispersion/repulsion, Coulomb, and polarization potential functions to the total intermolecular nonbonded energy of -12.0 kcal/mol are 8.6, -4.6, and -16.0 kcal/mol, respectively. It is clear that the surprisingly strong interaction between Li⁺ and methane is due primarily to the polarization of the methane by the small Li⁺ cation, which approaches quite near center of mass of the molecule. In structure II, the Li⁺ cannot approach as close to the center of mass of the molecule, and as a result the polarization effects and binding energies are correspondingly weaker.

Li⁺-Ethers

Quantum Chemistry. Complexes of Li⁺ with dimethyl ether and with DME in *ttt* and *tgt* conformations were investigated. The most important interaction of Li⁺ with the ethers involves the strong electrostatic attraction with the oxygen atoms. As illustrated in Figure 8, Li⁺ can approach closely to only one oxygen at a time in DME when it is in the *ttt* conformation. In the *tgt* conformation, however, both oxygen atoms are positioned to interact favorably with Li⁺ simultaneously. As given in Table 5, at the respective MP2 optimized geometries, the Li⁺-DME(*tgt*) complex binding energy is -63.40 kcal/mol with two

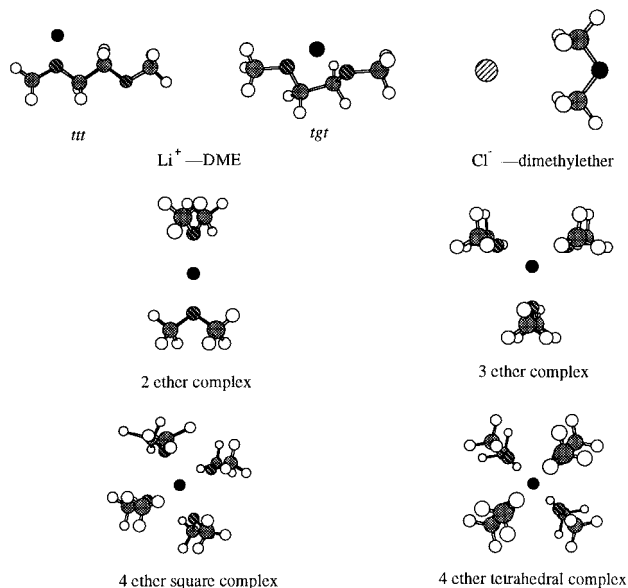


Figure 8. Geometries of the Li⁺-DME, and Li⁺-anion and Li⁺-multiple ether complexes investigated.

Li⁺-O distances of 1.87 Å, while the Li⁺-DME(*ttt*) complex binding energy is only -39.76 with an Li⁺-O distance of 1.84 Å. The Li⁺-DME(*ttt*) interaction is very similar to the Li⁺-dimethyl ether interaction, where a minimum energy of -39.7 kcal/mol at a separation of 1.84 Å was found. For isolated DME molecules, the *ttt* and *tgt* conformers differ in energy by less than 0.2 kcal/mol.²

Recently, Ray et al.²⁴ published measurements of the dissociation energy of the Li⁺-DME(*tgt*) complex using guided ion beam mass spectroscopy and obtained a value for ΔH°_0 of -57.6 ± 4.4 kcal/mol. In order to compare our results with experiment, we followed the same analysis used for the Li⁺-dimethyl ether complex. Harmonic normal mode vibration frequencies were computed at the SCF level using the [5s3p2d] and D95+** basis sets for lithium and DME, respectively. The frequencies were scaled by 0.9 to adjust for the effects of electron correlation and anharmonicity. Our resulting value of $\Delta H^{\circ}_0 = -61.2$ kcal/mol (D95+** ether basis set) is in reasonable agreement with the experimental value. If the ether basis set is improved to cc-pVTZ+sp, a $\Delta H^{\circ}_0 = -57.4$ kcal/mol is obtained using the smaller basis set frequencies. This value is in excellent agreement with experiment. Quantum chemistry calculations for the Li⁺-DME complex are also reported in ref 24. These were carried out in a similar manner to the present study, but used inferior quality basis sets. However, the resulting complex binding energies are similar to the ones reported herein, but the assignment of the vibrational modes is quite different.²⁵

The Li⁺-dimethyl ether (structure I and II) and Li⁺-DME (*ttt* and *tgt*) intermolecular nonbonded energy as a function of the Li⁺-O separation are shown in Figure 9. These values are relative to the distorted ether and include BSSE correction. For dimethyl ether (structure I) and the DME *tgt* complexes, the cation was moved along the C₂ axis. For the DME *ttt* complex, the cation was moved along constant line corresponding to the C₂ axis in dimethyl ether. For the dimethyl ether (structure II), the cation was moved along an Li⁺-O axis perpendicular to the C-O-C plane. Binding in this geometry is much weaker than is seen for structure I. For the Li⁺-DME(*ttt*) complexes only, the ether geometry was maintained as that found for the most stable complex. The Li⁺-dimethyl ether and Li⁺-DME(*ttt*) intermolecular nonbonded energies are nearly identical, while binding between Li⁺ and DME(*tgt*) is much stronger. Changing the Li⁺-O distance in the Li⁺-DME(*tgt*) results in

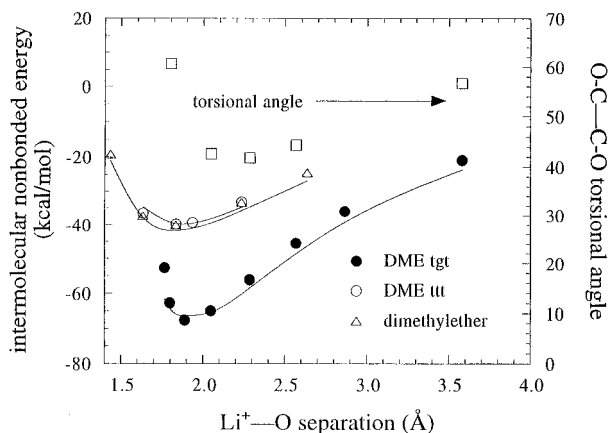


Figure 9. Intermolecular nonbonded energy for the Li^+ -dimethyl ether and Li^+ -DME complexes using $\text{Li}[5s3p2d]$ and D95+** ether basis sets. Also shown is the O-C-C-O torsional angle as a function of ion/molecule separation (filled circles). Lines for the DME (solid) and dimethyl ether (dashed) energies are values from the force field potential.

significant change in the O-C-C-O torsional angle, as shown in Figure 9. As the Li^+ -O distance decreases from large separations in the Li^+ -DME(*tgt*) complexes, significant distortion of the O-C-C-O torsional angle occurs. The torsional angle decreases (becomes nearer to eclipsed) because the binding energy gained by the increased interaction of both oxygen atoms with Li^+ is greater than the energy penalty associated with distorting the torsional angle. At even smaller separations, the torsional angle begins to increase as the complex become more sterically crowded. At the optimal complex geometry, the O-C-C-O torsional angle is about 26° smaller than is found for isolated DME(*tgt*), and the distortion energy of the ether is about 4.3 kcal/mol, which includes contributions from distortions of bond lengths and angles in addition to dihedrals.

In addition to ether complexes involving close Li^+ -O approaches, we investigated the interaction of Li^+ with the methyl group in dimethyl ether. The three structures examined are illustrated in Figure 6 (structures III-V). The intermolecular nonbonded energy as a function of the Li^+ -C separation is shown in Figure 7. In structure III the cation is moved along the C-O axis, while in structures IV and V it is moved along C-H axes. The binding of Li^+ to dimethyl ether in structures III-IV is an order of magnitude weaker than in structure I, which involves close interaction with the oxygen atom. Binding of Li^+ to the methyl group in dimethyl ether is weaker than the binding of Li^+ to methane, probably due to the net positive charge of the methyl group.

Potential Energy Functions. For the Li^+ -ether complexes, the potential parameters A_{LiO} , B_{LiO} , A_{LiC} , B_{LiC} , α_{O} , and α_{C} parameters were adjusted to so as to best reproduce the Li^+ -DME complex energies for *ttt* and *tgt* DME and the Li^+ -dimethyl ether complex energies for structures II-V. The A_{LiH} and B_{LiH} nonbonded parameters were taken from the fit to the Li^+ -methane complex energies. Because the Li^+ -methane complex energies were found to be rather insensitive to A_{LiC} , B_{LiC} , these were treated as adjustable in fitting the Li^+ -ether potential energy surfaces. The α_{H} and α_{C} parameters, although determined from fitting to Li^+ -methane complex energies, were treated as adjustable for the Li^+ -ether complexes because the structure of the ethers is quite different from methane, and hence the molecular polarizability may not be well described by the same effective atomic polarizabilities. The partial atomic charges were determined from quantum chemistry electrostatic potential calculations for dimethyl ether ($\text{C} = 0.10$, $\text{O} = -0.41$, $\text{H} = 0.035$), and those for DME were taken from previous work.¹

In parametrizing the force field, the greatest weight was given to reproducing the Li^+ -DME complex energies. We believe the most critical energies are around the DME *tgt* and *ttt* complex minima. Relatively little weight was given to reproducing the energies for the Li^+ -dimethyl ether structures II-IV because of the much weaker interactions involved. The resulting force field parameter values are given in Table 6. Good agreement of the force field potential energies with quantum chemistry can be seen for the DME complexes in Figure 9. The force field does a reasonable job reproducing the Li^+ -dimethyl ether (structure II) complex energies. The force field also reproduces the Li^+ -dimethyl ether (structure I) complex energies, which were not used in the parametrization of the force field, quite well. As a consequence, the binding of Li^+ with dimethyl ether predicted by the force field is in good agreement with experiment.²² This is in contrast to predictions obtained using a previous quantum chemistry based pairwise potential for cation/organic molecules.²⁶ In that work, calculations using much smaller basis sets yielded a binding of Li^+ with dimethyl ether of only 32.6 kcal/mol. Figure 7 reveals that the force field does a only a fair job in reproducing the Li^+ -dimethyl ether interactions for structure III-V. As these interactions are much weaker than those involving close interaction of the cation with the ether oxygen atoms, we believe the fit to be adequate.

Li^+ Interactions with Multiple Ethers

The two-body force field described above works well for describing interactions of a Li^+ ion with a single methane or ether molecule. Polarization effects are very important in these interactions; our force field predicts the contribution of the polarization terms of the potential to the complexes energies to be -25.5 and -59.5 kcal/mol for the lowest energy Li^+ -dimethyl ether and Li^+ -DME (*tgt*) complexes, respectively. These energies are comparable to the complex binding energies themselves. While the energetics of these interactions are accounted for by our two-body potential, the ether molecule is not actually polarized, i.e., no induced dipoles are introduced. Therefore, the interaction of an ether molecule or the ion with a second, third, etc., ether molecule added to the complex is not effected by the presence of the ion.

We have examined these mutual induction effects by investigating the interaction of Li^+ with one to four dimethyl ether molecules. The complexes studied are illustrated in Figure 8. Two four-ether complexes were considered: a square configuration, in which the ether oxygen atoms occupy the corners of a square with the cation in the center, and a tetrahedral arrangement, in which the oxygen atoms are tetrahedrally arrayed about the cation. Geometry optimizations were performed at the SCF level using a $[5s2p1d/\text{D95+**}]$ [Li^+ /ether] basis set. $\text{MP2}/[5s3p2d/\text{D95+**}]$ energies (relative to relaxed ethers at infinite separation), the ether distortion energies, and the intermolecular nonbonded energies are given in Table 7. Little difference was seen between SCF and MP2 complex energies except for the four-ether complexes, where a significant increase in the complex binding energy is observed at the MP2 level. Selected calculations indicated that BSSE effects are relatively small for the complexes compared to the total binding energies. The results of a recent experimental study²⁷ of these complexes are also presented in Table 7. The experimental values represent vibrational zero point energy corrected complex binding energies and generally are in good agreement with our quantum chemistry results. More detailed calculations for Li^+ interactions with multiple dimethyl ether molecules are in progress.

The intermolecular nonbonded energies from the force field potential are also given in Table 7; these energies are broken

TABLE 7: Interaction of Li⁺ with Multiple Dimethyl Ether Molecules

property	1 ether	2 ethers	3 ethers	4 ethers	
				square	tetrahedral
		Quantum Chemistry			
O–Li ⁺ separation ^a (Å)	1.82	1.85	1.92	2.10	2.01
complex energy ^b	-40.1	-74.1	-98.4	-108.4	-121.4
complex energy +ΔZPE ^{c,d}	-38.8	-71.6	-95.1		-116.5
	(-39.4)	(-70.5)	(-96.8)		(-119.6)
ether distortion energy	1.4	2.0	1.8	1.1	1.7
intermolecular nonbonded	-41.5	-76.1	-100.2	-109.5	-123.1
incremental energy ^c	-41.5	-34.6	-24.1	-9.3	-22.9
oxygen charge ^e	-0.58	-0.50	-0.40	-0.29	-0.31
		Force Field			
intermolecular nonbonded	-41.3	-80.7	-116.0	-137.2	-146.7
incremental energy	-41.3	-39.4	-35.3	-21.2	-30.7
intermolecular disp/rep	14.7	25.5	27.4	15.5	24.9
intermolecular electrostatic	-30.6	-57.5	-77.0	-82.8	-91.0
intermolecular polarization	-25.5	-48.7	-66.32	-69.9	-80.62
inter-ether energy		0.77	2.16	3.88	2.55

^a SCF optimized geometry. ^b MP2 values at SCF optimized geometries. Energies are in kcal/mol. ^c Includes vibrational zero point energy correction using frequencies from ref 27. ^d Experimental threshold from ref 27 in parentheses (comparable to vibrational zero point energy corrected complex energies). ^e Partial atomic charge for oxygen atoms from MP2 level Mulliken populations. The oxygen partial atomic charge for the relaxed single dimethyl ether molecule is -0.25.

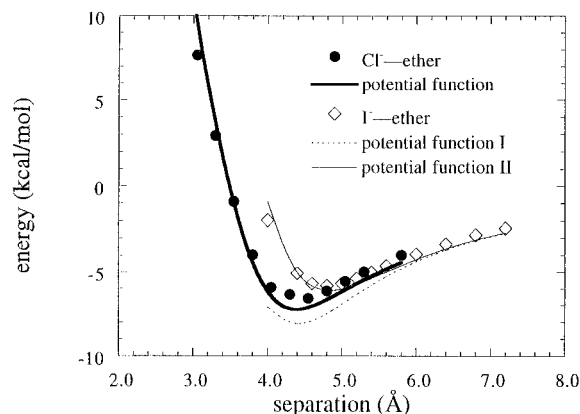


Figure 10. Intermolecular nonbonded energy for the Cl⁻-dimethyl ether and I⁻-dimethyl ether complexes using Cl[cc-pVTZ + 2s2p1d], I[4sp3d ECP], and D95+** ether basis sets. The solid lines for the complex energies are values from the force field potential.

down into dispersion/repulsion, electrostatic, and polarization contributions. The nonbonded energy for the ether complexes without the Li⁺ ion as predicted by the potential functions is also included in the table. This energy is a sum of the intermolecular dispersion/repulsion and electrostatic interactions between the ether molecules. Ether/ether dispersion/repulsion parameters were obtained from ref 1 and are summarized in Table 6. Finally, the dimethyl ether oxygen charge, as given by the MP2 Mulliken populations, is shown.

From the quantum chemistry calculations energies, it can be seen that the incremental binding energy decreases dramatically with the number of ether molecules in the complex, while the equilibrium O–Li⁺ separation increases. The oxygen partial charge is strongly perturbed by the presence of the Li⁺ ion, indicating that the ether molecules are strongly polarized by the Li⁺ ion. The decrease in the oxygen partial charge reveals that the polarization of the ether molecules decreases with the number of ethers in the complex. Hence, as ether molecules are added to the complex, the incremental binding energy decreases because (1) the effective polarization of the ethers, which results in favorable interactions with the Li⁺ ion, decreases and (2) polarization of the ethers results in unfavorable electrostatic interactions between ethers.

The force field potential predicts a much weaker dependence of the incremental binding energy on the number of ethers than is seen from the quantum chemistry calculations. The decrease

in the incremental binding energy predicted by the force field potential is due to the increase in distance between the ethers and the Li⁺ ion and unfavorable electrostatic interactions between the ethers. The latter effect is small for nonpolarized ethers, as indicated by the inter-ether energy in Table 7. Because the force field does not account for mutual induction effects, the unfavorable electrostatic interactions between ethers are dramatically underestimated, i.e., polarization effects are overestimated, and the binding energy for the multiple ether complexes is overestimated. For the four-ether (tetrahedral geometry) complex, the polarization potential energy must be scaled by 0.71 in order for the total binding energy to equal that from the quantum chemistry calculations. Reducing the strength of the polarization interactions by this factor also increases predicted equilibrium Li⁺–O distance to around 2.0 Å, in agreement with the quantum chemistry calculations for the four-ether (tetrahedral geometry) complex.

Cl⁻-Ether and I⁻-Ether Complexes

Quantum Chemistry. The interaction energies of Cl⁻ and I⁻ with a dimethyl ether molecule were examined for the structure shown in Figure 8. In this structure, the negatively charged anions can interact favorably with the hydrogen atoms, which have partial positive charges. The complex energy as a function of basis set for the Cl⁻ complex is given in Table 5. Augmenting the basis set beyond [cc-pVTZ+2s2p1d/D95+**] [Cl/ether] did not significantly change the complex energies. I⁻ complex energies were determined using a [4sp3d ECP/D95+**] [I/ether] basis set. Basis set superposition errors are around 1 kcal/mol for the anion complexes at the equilibrium separations. The [cc-pVTZ+2s2p1d/D95+**] [Cl/ether] basis set was used in determining the complex energy as a function of Cl⁻–O separation for [D95+*/D95+**] MP2 optimized geometries. For I⁻-dimethyl ether complexes, SCF optimizations using the [5sp4d1f ECP/D95+**] [I/ether] basis set were performed. For these structures, the anions were translated along the C₂ axis. The intermolecular nonbonded energies, relative to the distorted ether and anions at infinite separation, are shown in Figure 10. The binding energies of Cl⁻ and I⁻ to dimethyl ether are weaker by a factor of around 5 than the binding energies of Li⁺ to the ether. The binding energies of Cl⁻ and I⁻ to the ether are similar, although the equilibrium I⁻–O distance is greater than the Cl⁻–O distance due to the larger size of the I⁻ ion.

Potential Functions. For the Cl^- -ether interactions, the dispersion and repulsion parameters A_{XCl^-} , B_{XCl^-} , and C_{XCl^-} for $\text{X} = \text{C}, \text{H},$ and O were determined by using standard arithmetic (B_{XCl^-}) and geometric (A_{XCl^-} and C_{XCl^-}) combining rules with the $A_{\text{Cl}^-\text{Cl}^-}$, $B_{\text{Cl}^-\text{Cl}^-}$, and $C_{\text{Cl}^-\text{Cl}^-}$ values in Table 4 and the A_{XX} , B_{XX} , and C_{XX} parameters given in Table 6. The polarizabilities α_{C} , α_{O} , and α_{H} were treated as adjustable parameters in determining the corresponding D_{XCl^-} parameters. The Cl^- anion was assigned a polarizability of 4.39 \AA^3 . Although the α_{C} , α_{O} , and α_{H} parameters have been determined for Li^+ -ether interactions, the most favorable Cl^- -ether complex is of a very different geometry than the Li^+ -ether complex, as shown in Figure 8. As a consequence, the effective atomic polarizabilities previously determined for the Li^+ -ether complexes did a poor job in representing the Cl^- -ether complexes. The effective atomic polarizabilities and corresponding D parameters which best reproduce the Cl^- -ether complex energies are given in Table 6. Agreement between the force field potential and quantum chemistry energies for Cl^- -ether complexes is quite good, as can be seen in Figure 10. The polarization potential function contributes only 2.3 kcal/mol to the binding of Cl^- with dimethyl ether, whereas for the Li^+ -dimethyl ether complex the polarization interaction is around -25 kcal/mol. This difference is due to the ability of Li^+ to approach the ether molecule more closely. The equilibrium Li^+ -O separation is around 1.8 \AA in the Li^+ -ether complexes, while the closest Cl^- -H contacts are 3.2 \AA . The quantity $(3.2/1.8)^{-4}$ is about 0.1, comparable to the ratio of polarization energies found for the respective complexes.

For the I^- -dimethyl ether complex, using the same approach for determining A_{XI^-} , B_{XI^-} , and C_{XI^-} as described above for Cl^- -dimethyl ether, the α_{C} , α_{O} , and α_{H} effective atomic polarizabilities as determined for Cl^- -dimethyl ether, and an I^- dipole polarizability of 10.4 \AA^3 , yield the potential function labeled I in Figure 10. The potential function is too attractive compared to the quantum chemistry data. We believe this difference is due primarily to the force field underestimating steric interactions between I^- and the ether. The uncertainty in the I^- - I^- parameters is relatively large, and using simple combining rules for pairs differing in size as much as I^- and carbon, oxygen, and hydrogen is also a possible source of significant error. To improve the fit, we used the I^- - I^- parameters in Table 4 as a starting point and reduced $C_{\text{I}^-\text{I}^-}$ to $17\,000 \text{ kcal/mol \AA}^6$ and $B_{\text{I}^-\text{I}^-}$ to 1.834 \AA^{-1} for the purpose of determining B_{XI^-} , and C_{XI^-} . This makes I^- effectively larger for I^- -ether interactions than it would be using the simple combining rules with the unadjusted I^- - I^- parameters. The value of $A_{\text{I}^-\text{I}^-}$ was treated as an adjustable parameter. The best fit to the quantum chemistry data was found for a value of $A_{\text{I}^-\text{I}^-} = 35\,979 \text{ kcal/mol}$. The corresponding values of A_{XI^-} , B_{XI^-} , and C_{XI^-} are given in Table 6. The resulting potential function (II) is in reasonable agreement with the quantum chemistry data. As with Cl^- -dimethyl ether, the contribution of polarization interactions to the binding energy in the equilibrium geometry (-1.87 kcal/mol) is small compared to the Li^+ complexes.

Conclusions

Our studies of LiCl , LiI , and Li^+ , Cl^- and I^- complexes with ether molecules confirm that quantum chemistry can yield complex binding energies in good agreement with experiment, provided care is taken in employing adequate basis sets. This is particularly important for Li^+ , where the Li basis set must provide a good description of the core electrons and the where the binding of Li^+ to neutral molecules is strong because of the small size of the ion. The binding energy of the Li^+ -

methane complex is around 10 kcal/mol , while the binding of Li^+ to dimethyl ether and DME in the *ttt* conformation is around 40 kcal/mol . The binding of Li^+ to DME in the *tgt* conformation is greater than 60 kcal/mol because the Li^+ ion can interact favorably with both oxygen atoms in this configuration. In contrast, the bindings of Cl^- and I^- to dimethyl ether are only around $5-7 \text{ kcal/mol}$.

A simple force field with a two-body potential function for the polarization interactions was able to reproduce the binding energies of Li^+ with methane, dimethyl ether, and DME in both the *ttt* and *tgt* conformations and the binding of Cl^- and I^- to dimethyl ether. Polarization effects were found to contribute significantly to the binding of Li^+ to the neutral molecules in all cases. In contrast, the polarization interactions between Cl^- and I^- and dimethyl ether were found to be relatively weak in comparison to those for the Li^+ complexes and as a fraction of the binding energies in the anion-ether complexes.

When complexes of a single Li^+ cation with multiple dimethyl ether molecules were examined, it was found that the binding per ligand decreases substantially with the number of ligands. This effect is attributable to mutual induction effects within the complex. It was found that a simple force field with two-body potential functions representing induction or polarization effects could reproduce the *ab initio* complex energies quite well for the single-ligand complexes. The two-body force field failed to reproduce the observed decrease in binding per ligand with the number of ligands due to the failure of the force field to account for unfavorable ether-ether interactions resulting from polarization of the ether molecules.

Because of the apparent importance of mutual induction effects in cases involving multiple ligands, the ability our simple two-body force field to accurately represent polarization effects in bulk simulations of polymer electrolytes should be thoroughly investigated. Comparison of radial distribution functions for Li in POE/LiI melts from simulations using the two-body force field with results from neutron scattering measurements indicates reasonable agreement.²⁸ These simulations and experiments also confirm the importance of polarization effects.

Acknowledgment. G.D.S. is grateful to NASA (NCC-2701) and NSF (DMR-9624475) for support of this work.

References and Notes

- (1) Smith, G. D.; Jaffe, R. L.; Yoon, D. Y. *J. Phys. Chem.* **1993**, *97*, 12752.
- (2) Jaffe, R. L.; Smith, G. D.; Yoon, D. Y. *J. Phys. Chem.* **1993**, *97*, 12745.
- (3) Sorensen, R. A.; Liau, W. B.; Kesner, L.; Boyd, R. H. *Macromolecules* **1988**, *21*, 200.
- (4) Smith, G. D.; Jaffe, R. L.; Yoon, D. Y. *J. Am. Chem. Soc.* **1995**, *117*, 530.
- (5) Smith, G. D.; Jaffe, R. L.; Yoon, D. Y. *Polym. Prepr. (Am. Chem. Soc., Div. Polym. Chem.)* **1995**, *36*, 680.
- (6) Smith, G. D.; Yoon, D. Y.; Jaffe, R. L.; Colby, R. H.; Krishnamoorti, R.; Fetters, L. J. *Macromolecules* **1996**, *29*, 3462.
- (7) Rittner, E. S. *J. Chem. Phys.* **1951**, *19*, 1030.
- (8) Wheatley, R. J.; Hutson, J. M. *Mol. Phys.* **1995**, *84*, 879.
- (9) Rick, S. W.; Stuart, S. J.; Berne, B. J. *J. Chem. Phys.* **1994**, *101*, 6141.
- (10) Frisch, M. J.; Trucks, G. W.; Head-Gordon, M.; Gill, P. M. W.; Wong, M. W.; Foresman, J. B.; Johnson, B. G.; Schlegel, H. B.; Robb, M. A.; Replogle, E. S.; Gomperts, R.; Andres, J. L.; Raghavachari, K.; Binkley, J. S.; Gonzalez, C.; Martin, R. L.; Fox, D. J.; Defrees, D. J.; Baker, J.; Stewart, J. J. P.; Pople, J. A. *GAUSSIAN 92, Revision E.2.*; Gaussian, Inc.: Pittsburgh, PA, 1992.
- (11) Mulliken: A Computational Quantum Chemistry Program developed by J. E. Rice, H. Horn, B. H. Lengsfeld, A. D. McLean, J. T. Carter, E. S. Replogle, L. A. Barnes, S. A. Maluendes, G. C. Lie, M. Gutowski, W. E. Rudge, Stephan P. A. Sauer, R. Lindh, K. Andersson, T. S. Chevalier, P. O. Widmark, Djamel Bouzida, G. Pacansky, K. Singh, C. J. Gillan, P. Carnevali, William C. Swope, and B. Liu, Almaden Research Center, IBM Research Division, 650 Harry Road, San Jose, CA 95120-6099.

- (12) Langhoff, S. R.; Bauschlicher, C. W., Jr.; Partridge, H. *J. Chem. Phys.* **1986**, *84*, 1687.
- (13) Dunning, T. H.; Hay, P. J. *Methods of Electronic Structure Theory*, Schaefer, H. F., Ed.; Plenum Press: New York, 1977; pp 1–27.
- (14) Krishnan, R.; Binkley, J. S.; Seeger, R.; Pople, J. A. *J. Chem. Phys.* **1980**, *72*, 650.
- (15) Dunning, T. H. *J. Chem. Phys.* **1987**, *98*, 1007.
- (16) Stevens, W.; Jasien, P. G.; Krauss, M.; Basch, H. *Can. J. Chem.* **1992**, *70*, 612.
- (17) Huber, K. P.; Herzberg, G. *Molecular Spectra and Molecular Structure*; Van Nostrand Reinhold: New York, 1979.
- (18) Moore, C. E. *Atomic Energy Levels*; Natl. Stand. Ref. Data Serv. Natl. Bur. Stand. (U.S.) Circ. No. 467; U.S. GPO: Washington, DC, 1949.
- (19) Hotop, H.; Lineberger, W. C. *J. Phys. Chem. Ref. Data* **1975**, *4*, 530.
- (20) Ahlrichs, R.; Böhm, H. J.; Brode, S.; Tang, K. T.; Toennies, J. P. *J. Chem. Phys.* **1988**, *6290*.
- (21) Radzig, A. A.; Smirnov, B. M. *Reference Data on Atoms, Molecules and Ions*; Springer-Verlag: Berlin, 1985.
- (22) Woodin, R. L.; Beauchamp, J. L. *J. Am. Chem. Soc.* **1978**, *100*, 501.
- (23) Diercksen, G. H. F.; Kraemer, W. P.; Roos, B. O. *Theor. Chim. Acta* **1975**, *36*, 249.
- (24) Ray, D.; Feller, D.; More, M. B.; Glendening, E. D.; Armentrout, P. B. *J. Phys. Chem.* **1996**, *100*, 16116.
- (25) We assign the following vibration frequencies to transitional modes of the Li⁺–DME (*tgt*) complex: 154, 454, and 490 cm⁻¹.
- (26) Portmann, P.; Maruizumi, T.; Welti, M.; Badertscher, M.; Neszmelyi, A.; Simon, W.; Pretsch, E. *J. Chem. Phys.* **1987**, *87*, 493.
- (27) More, M. B.; Glendening, E. D.; Ray, D.; Feller, D.; Armentrout, P. B. *J. Phys. Chem.* **1996**, *100*, 1605.
- (28) Smith, G. D.; Borodin, O.; Pekny, M.; Annis, B.; Londono, D.; Jaffe, R. L. *Spectrochim. Acta*, in press.